Emerging 2D materials for tunneling field effect transistors

Materiales 2D emergentes para transistores de efecto de campo de efecto túnel

Nupur Navlakha[1], Leonard F. Register[2], Sanjay K. Banerjee[3]

Navlakha, N; Register, L.F; Banerjee, S.K. Emerging 2D materials for tunneling field effect transistors. *Tecnología en Marcha*. Vol. 36, special issue. June, 2023. IEEE Latin American Electron Devices Conference (LAEDC). Pág. 72-78.

https://doi.org/10.18845/tm.v36i6.6768

1 Microelectronics Research Center, Electrical and Computer Engineering, The University of Texas at Austin, Austin, TX-78758, United States.
Email: nupurnavlakha@utexas.edu
https://orcid.org/0000-0003-0673-7831
2 Microelectronics Research Center, Electrical and Computer Engineering, The University of Texas at Austin, Austin, TX-78758, United States.
Email: register@austin.utexas.edu
3 Microelectronics Research Center, Electrical and Computer Engineering, The University of Texas at Austin, Austin, TX-78758, United States.
Email: banerjee@ece.utexas.edu

Keywords

Tunnel field effect transistor; transitional metal dichalcogenides; type-III band alignment; heterostructure; black phosphorus; group IV Monochalcogenides.

Abstract

This work focuses on understanding the electronic properties of materials to enhance the performance of Tunnel Field Effect Transistor (TFET) through Density Functional Theory (DFT) simulations. Material selection prefers a *p*-type material with in-plane high density of state (DOS) (and low out-of-plane effective mass, m^*, where defined for many layer systems), and high valence band maxima (VBM) energy stacked with an *n*-type material with low conduction band minimum (CBM) energy (large electron affinity (EA)) that creates a broken or nearly broken band alignment and has low lattice mismatch. $SnSe_2$ is well-suited for an *n*-type 2D material due to high EA, while WSe_2, Black phosphorous (BP) and SnSe are explored for *p*-type materials. Bilayers consisting of monolayers of WSe_2 and $SnSe_2$ show a staggered but nearly broken band alignment (gap of 24 meV) and a high valence band DOS for WSe_2. BP-$SnSe_2$ shows a broken band alignment and benefits from a low lattice mismatch. SnSe-$SnSe_2$ shows the highest chemical stability, an optimal performance in terms of DOS of SnSe, tunability with an external field, and high VBM that also leads to a broken band alignment.

Palabras clave

Transistor de efecto de campo de túnel; dichaslcogenuros de metales de transición; alineación de bandas de tipo III; heteroestructura; fósforo negro; monocalcogenuros del grupo IV.

Resumen

Este trabajo se centra en comprender las propiedades electrónicas de los materiales para mejorar el rendimiento del transistor de efecto de campo de túnel (TFET) a través de simulaciones de la teoría funcional de la densidad (DFT). La selección de material prefiere un material de tipo *p* con alta densidad de estado (DOS) en el plano (y baja masa efectiva fuera del plano, m^*, donde se define para muchos sistemas de capas), y alta energía máxima de banda de valencia (VBM) apilado con un material de tipo *n* con energía mínima de banda de conducción baja (CBM) (afinidad electrónica grande (EA)) que crea una alineación de banda rota o casi rota y tiene un desajuste de red bajo. $SnSe_2$ es muy adecuado para un material 2D de tipo *n* debido a su alta EA, mientras que WSe_2, fósforo negro (BP) y SnSe se exploran para materiales de tipo *p*. Las bicapas que consisten en monocapas de WSe_2 y $SnSe_2$ muestran una alineación de bandas escalonada pero casi rota (brecha de 24 meV) y un DOS de banda de alta valencia para WSe_2. BP-$SnSe_2$ muestra una alineación de banda rota y se beneficia de un desajuste de red bajo. SnSe-$SnSe_2$ muestra la mayor estabilidad química, un rendimiento óptimo en términos de DOS de SnSe, sintonizabilidad con un campo externo y VBM alto que también conduce a una alineación de banda rota.

Introduction

2D-materials based Tunnel Field Effect Transistors (TFET) facilitate high interlayer tunneling on-currents (I_{on}) and gate controllability for short lateral channel lengths [1-6]. Although, graphene, transitional metal dichalcogenides (TMD), and their lateral and vertical heterostructures [2] have been investigated widely for TFETs [1,3,4], optimization to improve device design, reduce the off-current (I_{off}), improve I_{on} and sub-threshold swing (*SS*) and off current (I_{off}) is still needed.

Recently, WSe_2-$SnSe_2$ has shown promising results for vertical TFETs [5]. Moreover, WSe_2 shows ambipolar characteristics and can be replaced with a *p*-type material [1,3]. Use of a vertical hetero-bilayer that forms a broken or near broken band gap and requires less strain to form a lattice matched supercell is advantageous [3,4]. Here we explore other heterostructures for possible TFET application through Density Functional Theory (DFT) and compare results with those for WSe_2-$SnSe_2$. Results suggest that BP [7] and SnSe [8] can substitute for the *p*-type material in TFETs and is benefited with a higher strain tolerance, as well offer potential optoelectronics applications.

Computational method

Our calculations are performed using DFT with the projector-augmented wave method as implemented using the Vienna Ab initio Simulation Package [9]. The exchange-correlation interaction is included using the generalized gradient approximation developed by Perdew-Burke-Ernzerhof [10]. The lattice parameters of monolayers are optimized, and the calculated band gaps are consistent with previous literature [2,7,8,11]. The van der Waals (vdW) interactions are modeled using the OptB88 method [12]. The structures were fully relaxed with a force tolerance of 0.01 eV/Å. The energy cutoff was 400 eV, and the break criterion for the electronic self-consistent loop was 10^{-5} eV.

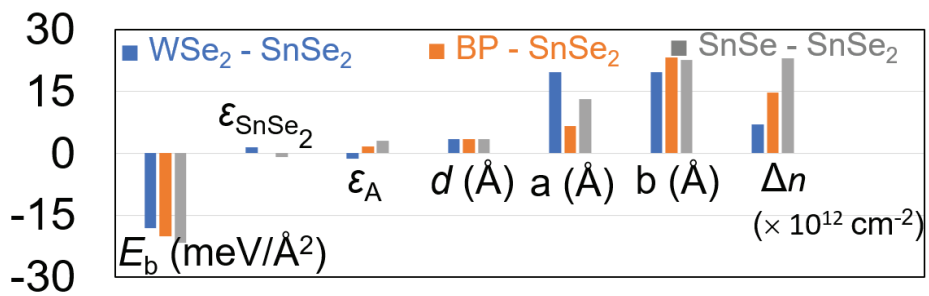

Figure 1. Comparison of binding energy per unit area (E_b), strain applied to create heterostructure (where ε and ε_A is the maximum strain applied in either *x* and *y* for $SnSe_2$, and material A (WSe_2, BP, SnSe), respectively, optimal interlayer distance (*d*), the dimensions of the lattice supercell created in the *x* (*a*) and *y* (*b*) directions, all in units of angstroms (Å), electron concentration (Δn) redistributed from Material A to $SnSe_2$ at zero applied field, in the heterolayers of WSe_2-$SnSe_2$, BP-$SnSe_2$, and SnSe-$SnSe_2$.

Results and discussion

Enhancing I_{on} requires a high Density of States (DOS) 2D material with high Valence Band Maxima (VBM) as the *p*-type material and an *n*-type material with a low Conduction Band Minima (CBM) or large Electron Affinity (EA) [3]. $SnSe_2$ shows high EA, while BP, WSe_2 and SnSe show a high VBM energy. We compare heterostructures of WSe_2-$SnSe_2$, BP-$SnSe_2$, and SnSe-$SnSe_2$. The binding energy per unit area (E_b) between the layers is calculated as $E_b = (E_{A/SnSe_2} - E_A - E_{SnSe_2})$ divided by the simulated heterostructure area, where $E_{A/SnSe_2}$, E_A, and E_{SnSe_2} are the total energy of the heterostructure, material A (WSe_2, BP, or SnSe), and $SnSe_2$, respectively, and Area is a ´ b, as defined in Fig. 1. The interlayer separation, *d*, is calculated as that which maximizes the magnitude of the (intrinsically negative) interlayer binding energy E_b, both provided Fig. 1. And the greater the magnitude of E_b, the more stable the structure. SnSe-$SnSe_2$, is the most stable followed in order by BP-$SnSe_2$ and WSe_2-$SnSe_2$. The lattice mismatch is the least for BP-$SnSe_2$ (1.6% in *y*-direction, zigzag and 0.3% in *x*, armchair)

and most for SnSe-$SnSe_2$ (-1% for $SnSe_2$, 2.9% in the *y*-direction of SnSe) (Fig. 1). Mismatch can result in disorder, which is difficult to control during fabrication and can impact the interlayer coupling [5]. However, the maximum strain in each layer is less than 3%.

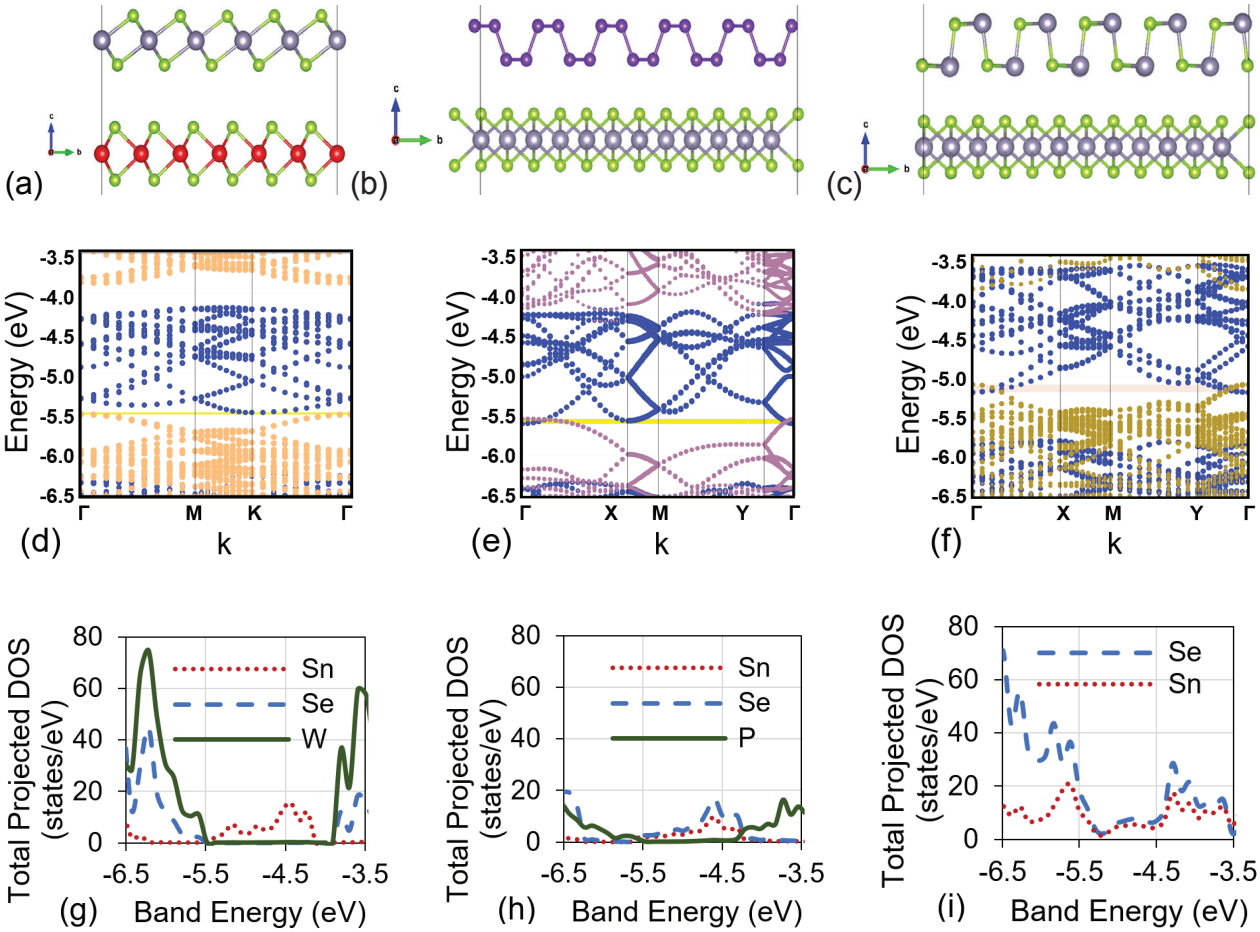

Figure 2. (a-c) The crystal structure in the *y-z* plane, (d-f) projected band structure, and (g-i) total projected density of state (DOS) of each material for WSe_2-$SnSe_2$, BP-$SnSe_2$, and SnSe-$SnSe_2$ in sequence. In (d-f), $SnSe_2$,WSe_2, BP, and SnSe atoms are represented in blue, cream, purple, green, respectively. All energies are referenced to vacuum level.

We stacked a 5x5, a √3x6, and a 2 √3x6 supercell of $SnSe_2$ with a 6x6 supercell of WSe_2, a 2x5 supercell of BP, and a 3x5 supercell of SnSe, respectively. (Fig. 2(a)-(c), respectively), resulting in supercells with dimensions shown in Fig. 1. The Bader charge analysis was used to obtain the electron redistribution from WSe_2, BP, and SnSe, which are 7.0 x 10^{12} cm^{-2}, 1.5 x 10^{13} cm^{-2} and 2.3 x 10^{13} cm^{-2}, respectively (Fig. 1). This charge transfer between the layers results in electrostatic interlayer coupling, which contributes to the aforementioned interlayer binding energy. Fig. 2 (d)-(f) shows that the CBM of each heterostructure originates from $SnSe_2$ and the VBM from material A. Fig. 2(d) shows the resulting Type II alignment for WSe_2-$SnSe_2$ with heterostructure band gap E_g = 24 meV, which can be tuned to a Type III alignment with a small potential. A Type III alignment is found for BP-$SnSe_2$ and SnSe-$SnSe_2$ with an overlap of the conduction and valence bands of 21 meV (Fig. 2(e)) and 31 meV (Fig. 2(f)), respectively. Fig. 2(g)-(i) shows the total atom-projected DOS for each material. The valence band DOS near the band-edge is highest for WSe_2-$SnSe_2$, still comparable for SnSe-$SnSe_2$, while that for BP-$SnSe_2$ is substantially smaller.

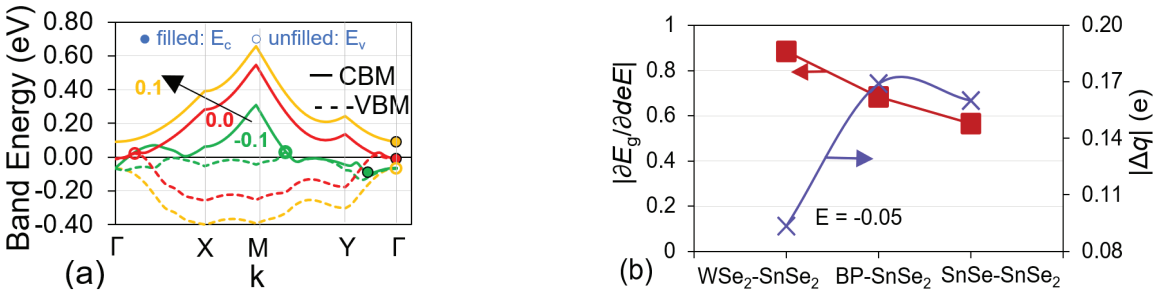

Figure 3. (a) The variation in the band structure associated with the CBM and VBM for SnSe-$SnSe_2$ with Electric field, *E* (-0.1 V/Å, 0.0 V/Å, 0.1 V/Å). All energies in (a) are referenced to DFT supplied fermi level. (b) Variation in band gap E_g with applied external electric field *E* (-0.05 V/Å) adjusted for the interlayer separation *d* and electron charge magnituded *e*, $|\partial E_g/\partial(deE)|$ and the change in electron distribution (Δq) in Material A (opposite that in $SnSe_2$) due to an an applied external electric field of *E* of -0.05 V/Å. Note that in the absence of field screening within the the bilayer, $|\partial E_g/\partial(deE)|$ would be approximately unity.

Minimizing the sub-threshold swing requires maximizing gate efficiency, which can be quantified as change in the band overlap with applied voltage [13], where a higher change in E_g with a lower bias is desirable. The impact of external field on the band alignment can be observed in Fig. 3(a), where a positive field is directed from Material A to $SnSe_2$. For a 0.1 V/Å, SnSe-$SnSe_2$ shows a Type-II band alignment with a direct band gap. We compared the change in band gap with a field of –0.05 V/Å, which is equivalent to an interlayer potential difference of ~0.17 V between the layers for each heterostructure. Fig. 3(b) shows the variation is maximum for WSe_2-$SnSe_2$, followed by BP-$SnSe_2$, and SnSe-$SnSe_2$. The change in the charge distribution with applied external field is the largest for BP-$SnSe_2$. This result shows a possibility for better current control for this heterostructure as compared to the others. The material requirements and the results obtained here suggest SnSe-$SnSe_2$ could be utilized as a channel material for TFETs. Other Group-IV monochalcogenides [8] also could be explored as the *p*-type material for TFETs.

Conclusion

The work emphasizes on the need to replace the devices with new material system. The objective is to explore $SnSe_2$ heterostructures that can operate as tunneling transistors. Comparing WSe_2-$SnSe_2$, BP-$SnSe_2$, and SnSe-$SnSe_2$ shows that SnSe-$SnSe_2$ provides optimal performance in terms of stable structure, high DOS, tunability with electric field, and a broken band alignment that nominates it for being investigated at device level.

Acknowledgment

We thank National Nanotechnology Coordinated Infrastructure (NNCI), which is supported by the National Science Foundation under the Grant ECCS-2025227. We also acknowledge the Texas Advanced Computing Center (TACC) at The University of Texas at Austin for providing high performance computing resources for this work.

References

[1] C. Gong, et al., “Band alignment of two-dimensional transition metal dichalcogenides: Application in tunnel field effect transistors”, Applied Physics Letters 103, 53513 (2013).

[2] Zhang, Chenxi, et al. “Systematic study of electronic structure and band alignment of monolayer transition metal dichalcogenides in Van der Waals heterostructures.” 2D Materials 4. 1 (2016): 015026.

[3] Chen, F.W., Ilatikhameneh, H., Klimeck, G., Chen, Z. and Rahman, R., 2016. Configurable electrostatically doped high performance bilayer graphene tunnel FET. IEEE Journal of the Electron Devices Society, 4(3), pp.124-128.

[4] Cao, Wei, et al. "Designing band-to-band tunneling field-effect transistors with 2D semiconductors for next-generation low-power VLSI." 2015 IEEE International Electron Devices Meeting, 2015.

[5] Cao, J., Logoteta, D., Pala, M.G. and Cresti, A., 2018. Impact of momentum mismatch on 2D van der Waals tunnel field-effect transistors. Journal of Physics D: Applied Physics, 51(5), p.055102.

[6] Oliva, Nicolò, et al. "WSe 2/SnSe 2 vdW heterojunction Tunnel FET with subthermionic characteristic and MOSFET co-integrated on same WSe_2 flake." npj 2D Materials and Applications 4.1 (2020): 1-8.

[7] Ameen, Tarek A., et al. "Few-layer phosphorene: An ideal 2D material for tunnel transistors." Scientific reports 6.1 (2016): 1-7.

[8] Li, Hong, Peipei Xu, and Jing Lu. "Sub-10 nm tunneling field-effect transistors based on monolayer group IV mono-chalcogenides." Nanoscale 11.48 (2019): 23392-23401.

[9] Kresse, Georg, and Jürgen Furthmüller. "Efficient iterative schemes for ab initio total-energy calculations using a plane-wave basis set." Physical review B 54.16 (1996): 11169.

[10] Shafique, A., Samad, A. and Shin, Y.H., 2017. Ultra-low lattice thermal conductivity and high carrier mobility of monolayer SnS_2 and $SnSe_2$: a first principles study. Physical Chemistry Chemical Physics, 19(31), pp.20677-20683.

[11] Perdew, John P., Kieron Burke, and Yue Wang. "Generalized gradient approximation for the exchange-correlation hole of a many-electron system." Physical review B 54.23 (1996): 16533.

[12] Klimeš, Jiří, David R. Bowler, and Angelos Michaelides. "Van der Waals density functionals applied to solids." Physical Review B 83.19 (2011): 195131.

[13] Agarwal, S., Teherani, J.T., Hoyt, J.L., Antoniadis, D.A. and Yablonovitch, E., 2014. Engineering the electron–hole bilayer tunneling field-effect transistor. IEEE Transactions on Electron Devices, 61(5), pp.1599-1606

TEXAS
The University of Texas at Austin

LAEDC 2022 LATIN AMERICAN ELECTRON DEVICES CONFERENCE

Emerging 2D Materials for Tunneling Field Effect Transistors

Nupur Navlakha*, Leonard F. Register, and Sanjay K. Banerjee
Microelectronics Research Center, Electrical and Computer Engineering,
The University of Texas at Austin, Austin, TX-78758, United States
nupurnavlakha@utexas.edu*, register@austin.utexas.edu, and banerjee@ece.utexas.edu

Introduction

2D material based heterostructure as Vertical Tunnel Field Effect Transistor (TFET), FIG. 1:

- High interlayer tunneling on-currents (I_{on}) and gate controllability
- Non-dangling bond reduces the performance degradation occurring due to traps in lateral heterojunction based TFETs
- Need new material systems for enhanced performance

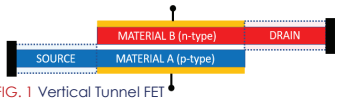

FIG. 1 Vertical Tunnel FET

Material requirement/selection for enhanced performance:

- Bilayer with a near broken or broken band gap
- Requires less strain to form a lattice matched supercell
- High Density of States (DOS) 2D material with high Valence Band Maxima (VBM) energy as the *p*-type material
- *n*-type material with a low Conduction Band Minima (CBM) energy or large Electron Affinity (EA)

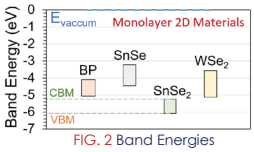

FIG. 2 Band Energies

Material selection (FIG. 2)
$SnSe_2$: High EA (*n*-type)
WSe_2, SnSe, BP : High VBM (*p*-type)
Bilayers for comparison:
WSe_2 - $SnSe_2$, BP - $SnSe_2$, SnSe - $SnSe_2$

Materials and Methods

- Density Functional Theory (DFT) calculations performed using Vienna Ab initio Simulation Package (VASP).
- Projector-augmented wave (PAW), Exchange-correlation interaction - Generalized Gradient Approximation (GGA) developed by Perdew-Burke-Ernzerhof (PBE)
- van der Waals interactions - OptB88 functional method

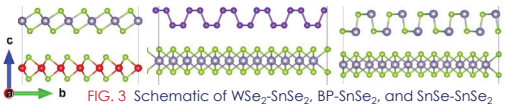

FIG. 3 Schematic of WSe_2-$SnSe_2$, BP-$SnSe_2$, and SnSe-$SnSe_2$

- Stacked a 5×5, a √3×6, and a 2√3×6 supercell of $SnSe_2$ with a 6×6 supercell of WSe_2, a 2×5 supercell of BP, and a 3×5 supercell of SnSe, respectively (FIG. 3).

Results and Discussion

- Greater the magnitude of E_b, more stable the structure. Stability: SnSe-$SnSe_2$ > BP-$SnSe_2$ > WSe_2 -$SnSe_2$ (FIG. 4).
- Lattice mismatch: SnSe-$SnSe_2$ > WSe_2 -$SnSe_2$ > BP-$SnSe_2$
- Higher charge transfer between layers → better interlayer coupling: SnSe-$SnSe_2$ > BP-$SnSe_2$ > WSe_2 -$SnSe_2$

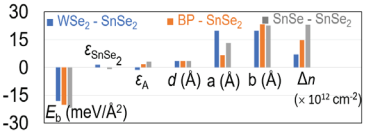

FIG. 4 Parameters of WSe_2-$SnSe_2$, BP-$SnSe_2$, and SnSe-$SnSe_2$ bilayers
1. Binding energy per unit area (E_b), $E_b = (E_{A/SnSe_2} - E_A - E_{SnSe_2})$, 2. Strain applied to create heterostructure (where ε and ε_A is the maximum strain applied in either x and y for $SnSe_2$, and material A (WSe_2, BP, SnSe), respectively, 3. Optimal interlayer distance (*d*), 4. The dimensions of the lattice supercell created in the x (*a*) and y (*b*) directions, all in units of angstroms (Å), 5. Electron concentration (Δ*n*) redistributed from Material A to $SnSe_2$ at zero applied field.

- Type II alignment for WSe_2-$SnSe_2$ with heterostructure band gap E_g = 24 meV (FIG. 5(a))
- Type III alignment for BP-$SnSe_2$ with an overlap of 21 meV of the conduction and valence bands (FIG. 5(b))
- Type III alignment for SnSe-$SnSe_2$ with an overlap of 31 meV of the conduction and valence bands (FIG. 5(c)).

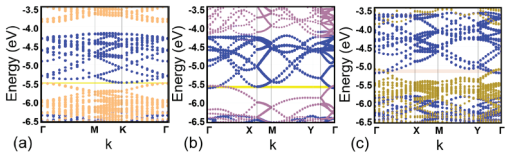

FIG. 5 Band Energies of (a) WSe_2-$SnSe_2$, (b) BP-$SnSe_2$, and (c) SnSe-$SnSe_2$

- The valence band DOS near the band-edge is highest for WSe_2-$SnSe_2$, still comparable for SnSe-$SnSe_2$, while that for BP-$SnSe_2$ is substantially smaller (FIG. 6).
- Analysis with an external field shows tunability in all bilayers

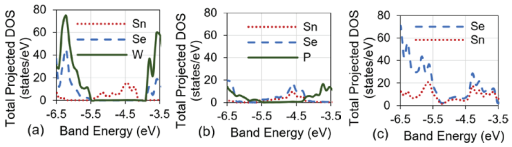

FIG. 6 Projected DOS for (a) WSe_2-$SnSe_2$, (b) BP-$SnSe_2$, and (c) SnSe-$SnSe_2$

Conclusions / Next Steps

- Properties of bilayer material system with nearly broken or broken band gap are compared for TFET operation where,
- WSe_2 -$SnSe_2$ is beneficial due to high DOS and tunes into a broken band gap with a small external field
- BP- $SnSe_2$ has low lattice mismatch
- SnSe-$SnSe_2$ provides optimal performance in terms of most stable structure, high DOS, band tunability with electric field
- SnSe-$SnSe_2$ shows potential to investigate at device level.
- Other Group IV Monochalcogenides can be explored as *p*-type material in TFET device.

IEEE Advancing Technology for Humanity

2022 IEEE Latin American Electron Devices Conference (LAEDC)

ELECTRON DEVICES SOCIETY

Illustration 1. Presented Poster at LAEDC 2022.